






ORIGINAL RESEARCH PAPER |  Open Access |  

# Co-optimisation of wind farm micro-siting and cabling layouts

A. Al Shereiqi , B. Mohandes, A. Al-Hinai , M. Bakhtvar, R. Al-Abri, M. S. El Moursi, M. Albadi

First published: 22 March 2021 |  
<https://doi.org/10.1049/rpg2.12154>

## Abstract

Wind farm layout optimisation (WFLO) is carried out in this study considering the wake effect, and cabling connections and losses. The wind farm micro-siting optimisation problem is formulated with the aid of Jensen's wake model. Cabling between the wind turbines and the point of common coupling is an important aspect of the wind farm design as it affects the capital investment as well as income over the lifetime of the wind farm. The cabling layout must satisfy the connection of the wind turbines to the point of common coupling in such a way that the total cable length is reduced while reliability is maintained. Introducing the cabling layout optimisation to the WFLO, further complicates the optimisation problem. An integrated tool is developed to optimise the wind farm layout and cabling simultaneously. The main contribution of this



Figures References Related Infor

## Metrics



## Details

© 2021 The Authors. *IET Renewable Power Generation* published by John Wiley & Sons Ltd on behalf of The Institution of Engineering and Technology

This is an open access article under the terms of the [Creative Commons Attribution](#) License, which permits use, distribution and reproduction in any medium, provided the original work is properly cited.

## Research Funding

Sultan Qaboos

work is the development of an integrated tool that maximizes the energy production of the wind farm via optimal allocation of wind turbines with optimal cable routing. This tool considers the capital cost of wind turbines and cabling, wind farm power production, and power losses in the cabling over the lifetime of the wind farm. The proposed co-optimisation problem is solved using genetic algorithm. The decision variables are the wind farm layout, cable paths and sizes, and the location of the point of common coupling within the land perimeter. A case study incorporating a multi-speed and multi-direction wind profile is carried out to demonstrate the applicability of the proposed approach. Moreover, the proposed methodology is compared to the separate optimisation method where the WFLO and cabling optimisation are solved sequentially with two separate steps. It is shown that the co-optimisation method is superior in terms of cable power losses, overall wind farm cost, and compactness (land use).

University. Grant  
Number: HMTF  
(SR/ENG/ECE/17/01)

## Publication History

**Issue Online:**  
14 May 2021

**Version of Record  
online:**  
22 March 2021

**Manuscript accepted:**  
03 March 2021

**Manuscript revised:**  
27 February 2021

## 1 INTRODUCTION

The integration of renewable resources in power generation, and wind energy in particular, has become a primary focus in investments in the power generation sector. Wind farms (WFs) play a significant role in satisfying the demand for energy, but constructing a WF still involves technical challenges, as well as cost implications. Wind profile is crucial in defining the turbine's capability in energy production. For instance, the cubical relationship between wind speed and wind output power means that any deviation in wind speed leads to a severe impact on the turbine's output power and, consequently, the system's performance [1].

and, consequently, the system's performance [1]. Therefore, a hierarchy of the turbine's specification, wind profile, and site geography of the WF are required to build a farm that utilizes resources efficiently and provides a better performance. One of the main challenges in WF design is the allocation of wind turbines with the aim of decreasing the ambiguity in output power [2].

The main steps involved in the design of a WF are as follows: site identification, technical and economic analysis, regulatory compliance, micro-siting, and construction [3]. In general, the wind farm layout optimisation (WFLO) problem is complex because many factors have to be involved. The wake effect in the farm is one of the main factors that affect the WF output power. The wake effect is the change in the effective wind speed that powers downstream turbines, as a result of the turbulence caused by upstream turbines. The complexity of the WFLO problem necessitates the use of optimisation techniques to obtain an optimal layout. The WFLO problem has been tackled in the literature with different fitness functions and different optimisation techniques. Heuristic techniques demonstrate superior performance compared with analytical optimisation methods, even for optimising a simple objective such as maximizing the farm's output power [4]. According to the literature, genetic algorithm (GA) is one of the heuristic methods commonly used to solve such a mixed-integer problem. This is due to its ability to avoid local optima and its high likelihood of locating global optima [5, 6]. The authors in [7] used GA to find the optimal number and location of wind turbines and obtaining optimal power production.

The wake effect has been introduced in the WFLO

problem using different models. Various models have been developed to represent the wake effect, namely, Gaussian's [8, 9], Jensen's [10, 11], Larsen's [12], and Frandsen's [13]. These models differ in their level of complexity and, therefore, computational burden. An early attempt to use Jensen's model in WFLO was carried out by Mosetti et al. [7, 14] in 1993, employing GA to minimize the cost per unit energy produced. They investigated the problem for different wind scenarios with varying complexities. The wind scenarios commonly evaluated in the literature comprise wind with a constant speed and direction, wind with a constant speed but variable direction, and wind with a variable speed and variable direction. Grady et al. [15] improved the WFLO using the same objective function, the same wake-effect model, and the same grid strategy of Mosetti et al. [14]. The improvement in results is attributed to the usage of different GA parameters. Most of the published research work [16-18] for solving WF optimisation used Jensen's wake-effect model that assumes a uniform velocity inside the wake cone.

A recent study [19] used Jensen's wake-effect model and optimised the layout using the binary real coded GA (BRCGA) based on a local search approach. The underlying principle is to find the turbine location with the power output of each turbine. The GA solution was improved using the local search technique to find the optimal solution near the solution found by BRCGA. The researchers tested their method on two wind scenarios: wind with multiple directions and multiple speeds and wind with multiple directions but constant speed. They demonstrated that using BRCGA, the output power is slightly increased compared with the results achieved by [15] but incurs a higher computational burden. Similar observation is reported by [20]. Particle swarm

optimisation (PSO) was used in [21] to solve a multi-objective WFLO problem by maximizing the power output and minimizing the costs. The optimisation formulation constraints are the dimensions of the land lot and a clearing distance of eight times the rotor diameter between any two wind turbines, according to the industry standard.

Heuristic optimisation techniques are most commonly used to tackle such WFLO problems [9, 22]. In [23], a fast approach is developed for optimising the layout of a large WF, whereas the approach in [24] is applicable for a WF with few wind turbines. Other techniques such as quadratic integer programming, multi-population GA, and non-linear programming were used in [25], [26], and [27] respectively. A heuristic ant-colony optimisation algorithm is presented in [28] for the layout optimisation of a WF with eight turbines and a cost-integrated model. Amaral et al.[29] used GA and PSO in solving offshore WFLO and compare the performance of each approach. It has been concluded that PSO performs faster while GA yields better results. A comprehensive review is presented in [30] for the GA, PSO, and fuzzy methods. These heuristic techniques are widely used in the optimal design of hybrid renewable energy systems. The algorithm and mechanism of GA are explained, in detail, in [31]. GA is widely used in solving WFLO problem, which represents 75% of the WFLO studies [32]. Thus, according to the literature surveyed; to solve this nonlinear, constrained optimisation problem, most of the previous studies used heuristic algorithms. Therefore, GA is adopted in this paper to solve the WFLO problem.

Cabling work is a significant part of the total cost of a WF construction. Cabling work includes small cabling

among wind turbines and a large collector cable that connects the wind turbines to the point of common coupling (PCC). During WF construction, cabling between the wind turbines is one of the debatable design tasks. As stated in [33], the installation and capital cost of the cabling work significantly contributes to the total cost of the project. In addition, energy losses constitute an operation cost, which affects the long-term financial profitability of the project. Hence, cable work should not be neglected. Simple techniques such as geometric programming were used in [34] to obtain the optimal electrical layout. The first attempts in WF cabling adopted a greedy algorithm [35]. The greedy algorithm starts by adding a turbine to a location that provides maximum power output. This process is repeated for all the turbines while considering the wake effect of the existing turbines. The process ends when the maximum number of turbines is reached [36]. This algorithm connects each turbine to its closest neighbour, which is not necessarily optimal. In other words, the solution provided by the greedy algorithm is far from optimal because each step depends on the formation created by the preceding step and lacks a holistic view of the land layout.

A mixed-integer linear program (MILP) is used in [37] to optimise the WF's electrical network. The optimisation process takes into account the cost of cable material, civil works (i.e. trenches), and energy losses. However, the optimal location and number of turbines is out of their scope. The authors in [35, 38] optimise the cabling between the wind turbines while the number and layout were optimised a priori. The authors justify optimising the number and layout WTs separately and beforehand by highlighting the large cost of wind turbines in comparison with the cabling cost. Nonetheless, the cost

comparison with the cabling cost. Nonetheless, the cost and energy losses that correlated with the cable work must be incorporated in the WFLO problem. Gonzalez et al. [39] optimise the cable work using GA, with the objective of minimizing the capital cost of a WF, inclusive of the costs of transformers, substations, and cables. The cable losses and wake effect are not included in this model. Furthermore, GA was used in [40, 41] to optimise the levelised production cost to find the optimal electrical system design for a fixed number of turbines. Lehmann et al. [42] use simulated annealing (SA) for solving the minimum cost problem in the whole WF cabling and comparing the performance of this approach with MILP. However, the authors do not incorporate cable losses in their model. Besides, different cable routing scenarios are investigated in [43] but with a fixed number of turbines. The implementation of GA is more efficient compared to the MILP in solving the WFLO problems. Most of the previous studies used heuristic optimisation techniques (i.e GA) due to the complexity of the problem. Furthermore, GA has the ability to get the global optimal solution in a reasonable computational time. In virtue of the previous studies, in this paper, the integrated optimisation approach used heuristic optimisation techniques to get an optimal cabling layout and optimal wind turbines layout simultaneously.

As observed in the aforementioned studies, none of the works in the literature incorporate cabling work in the WFLO problem. The two problems are tackled sequentially, rather than simultaneously. This is based on the claim that the WF construction cost is disproportionately larger than the cost of cabling. However, cabling work constitutes a considerable part of WF cost [37, 39] and has a sustained effect on the

WF's operation cost. This sustained effect is associated with the wind farm power losses during the farm's entire lifespan. The electrical infrastructure that includes cabling and substations represents roughly 15–30% of the total capital cost of the WF [44]. Hence, this study tackles this problem by co-optimising the layout of a WF and cabling. Jensen's wake-effect model is used to formulate the WFLO problem. A model for WF cabling is developed and included in the WFLO which considers active power losses, costs, and lengths of the main cable and service cables. The optimisation problem is solved using GA to obtain the minimal cost per unit power of the entire WF. The proposed methodology enables to define the optimal wind turbine layout, cabling layout, and location of the PCC. This paper is different from [37] as it uses GA, does not fix wind turbines, does tackle the problem simultaneously instead of separate optimisation problems.

A case study is carried out to demonstrate the proposed WFLO method. Thus, the paper highlights the following points:

- An integrated tool for wind farm layout with cables routes is developed.
- Jensen's wake-effect model is used as a parameter in the wind farm layout.
- Multi-speed and multi-direction wind scenario is used to test the developed approach.
- The optimisation yields an optimal number and location of wind turbines, optimal routes of cables and optimal location of the point of common coupling.
- The results for co-optimisation and separate optimisation of wind farm and cables routes are compared and reported.

The remaining sections in this paper are organized as



The remaining sections in this paper are organized as follows: Section 2 formulates the optimisation problem including the wake-effect model and optimal cable design. Section 3 carries out a simulation for a case study with multi-speed and multi-direction using co-optimisation and separate optimisation for WF micro-siting and cabling connections. The main factors considered in this study among all the other factors that affect WF layout are characteristic of the installed wind turbines, magnitude and direction of wind speed, wake effect, active power losses of cables, and power output from the WF. Finally, Section 4 shows another case for a site in south of Oman, and Section 5 presents the study conclusion.

## 2 PROBLEM FORMULATION

This study tackles the WFLO problem by co-optimising the wind turbine layout, cabling layout, and location of the PCC. The co-optimisation features a single-level optimisation process with the objective of minimizing the cost of energy. The objective function considers the active power losses in the WT connection cables. This section presents the problem formulation with main factors embedded in this WFLO problem. The proposed methodology is also benchmarked using the previous case studies.

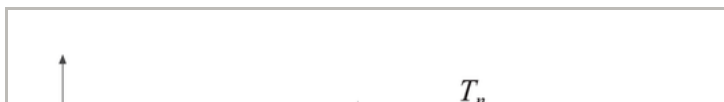
### 2.1 Jensen's wake-effect model

The wake effect is the effect of upstream wind turbines on the speed of wind that reaches downstream turbines. A mass of air flowing has kinetic energy which is proportional to the air mass and flow rate (i.e. wind speed). Part of the kinetic energy is extracted by wind turbines when air passes through its blades. Therefore, there is a reduction in the energy content of air behind

the turbine. This reduction exhibits as reduced speed of the air after it passes through the wind turbine blades. However, the further behind the turbine, the more the speed of air recovers to its original value. Accordingly, an upstream wind turbine can affect the wind speed on downstream turbines. This aerodynamic interaction between wind turbines has been the subject of many studies. Jensen's model is based on the energy momentum concept and characterized by its dependence on the distance behind the rotor and linear expanding wake with the velocity deficit. It is the most common model in the literature [7, 45] due to its simplicity and relatively good accuracy, particularly for a far wake zone which is equal to or more than  $(D_r)0$  length [46].

Jensen's model is used in this paper to model the wake effect in WF. An illustration of Jensen's model is shown in Figure 1. It is representing a single wake of a turbine. The  $(T_i)$  located at  $(x_i, y_i)$  and  $(T_n)$  located at  $(x_n, y_n)$  are the upstream and downstream turbines, respectively. The wake flow is axis-symmetric and linear which depends only on the distance behind the rotor toward the wind direction, as shown in the blue dashed line with a radius of  $(r_{in})$ . In this model, the wind speed at  $T_n$  is give as:

$$v_n = v_0 \left[ 1 - \sqrt{\sum_{i=1}^N \left[ \frac{2a}{\left(1 + \frac{\alpha y_{in}}{r_{in}}\right)^2} \right]^2} \right] \quad (1)$$



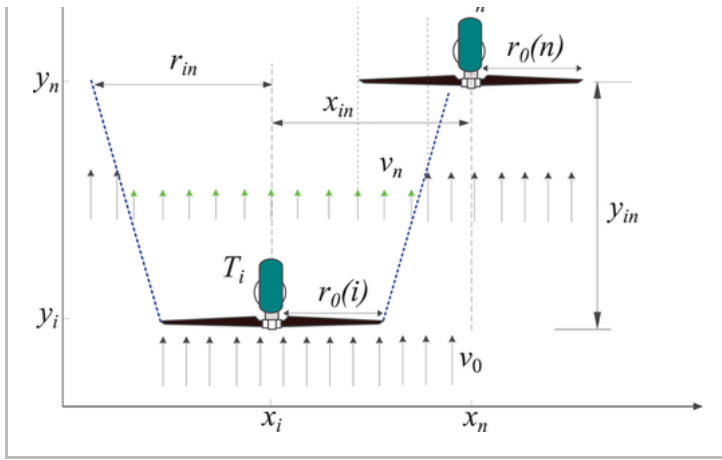


**FIGURE 1** [Open in figure viewer](#) | [↓ PowerPoint](#)

Principle of Jensen's wake-effect model (top view of the wind farm)

where

$$r_{in} = \alpha y_{in} + r_0(i)$$

The dimensionless scalar ( $\alpha$ ), known as a decay constant, defines the growth of wake width with distance which is given by Equation (2). The fractional decrease in wind speed between the free stream wind speed ( $v_0$ ) and the turbine is presented by the axial induction factor ( $a$ ) as depicted in Equation (3). Based on the turbine hub height, surface roughness and thrust coefficient, the values of the decay-constant and the axial induction factor can be calculated as 0.094 and 0.3268, respectively.

$$\alpha = \frac{1}{2 \ln\left(\frac{H_{wt}}{z_0}\right)}$$

(2)

$$a = 0.5[1 - \sqrt{1 - C_t}]$$

(3)

Thus, the reduction in wind speed at ( $T_n$ ) for multiple turbines in the farm is represented mathematically using Equation (4):

$$v_n = v_0 \left[ 1 - \sqrt{\sum_{i=1}^N \left[ \frac{[1 - \sqrt{1 - C_t}]^2}{r} \right]} \right]$$

(4)

where

$$r = \left[ 1 + \frac{y_{in}}{2 * \ln\left(\frac{H_{wt}}{z_0}\right)(\alpha * y_{in} + r_0(i))} \right]^2$$

A linearly expanding disc analogy is used in Jensen's wake model. Accordingly, the area of influence of wake effect behind a turbine expands by moving away from it. However, the severity of this influence also drops by moving away from the turbine. For example, assuming turbines diameter of 40 m, a downstream turbine ( $T_n$ ) 200 m away from the upstream turbine ( $T_i$ ) and fully affected by its wake, experiences a velocity deficit of 29.66% compared to the velocity in the upstream turbine. Moreover, using turbines diameter of 60 m with 200 m spacing leads to a velocity deficit of 34.06% in the speed reaching the turbine ( $T_n$ ).

As implied in the Jensen model, only a part of a turbine swept area may be affected by the wake. A turbine that

is partially aerodynamically affected by the upstream turbine is said to be under the shadowing of the upstream turbine. Shadowing is a measure of the degree of overlap between the area swept by the affected downstream rotor and the area spanned by the wake's shadow cone. The shadowing ratio ( $A_x$ ) is given by Equation (5). The ratio ( $A_x$ ) is 0 if there is no wake effect. Furthermore, a ratio of 1 means that the downstream wind turbine rotor is totally inside the wake. Whether the turbine is under the wake effect ( $\omega_{\text{wake}}$ ) or not is specified according to the conditions given by Equation (6). Thus, the corresponding wind speed ( $v_0$ ) approaching downstream wind turbine ( $T_n$ ) is expressed by Equation (7).

$$A_x = \left\{ \frac{r_0(i)^2 \cos^{-1} \left( \frac{x_{\text{in}}^2 + r_0(i)^2 - r_{\text{in}}^2}{2x_{\text{in}}r_0(i)} \right) - \hat{h}}{\pi(r_0(i))^2} + \frac{r_{\text{in}}^2 \cos^{-1} \left( \frac{x_{\text{in}}^2 - r_0(i)^2 + r_{\text{in}}^2}{2x_{\text{in}}r_{\text{in}}} \right)}{\pi(r_0(i))^2} \right\} \quad (5)$$

where

$$\hat{h} = \{0.5[(-x_{\text{in}} + r_0(i) + r_{\text{in}})(x_{\text{in}} + r_0(i) - r_{\text{in}}) \times (x_{\text{in}} - r_0(i) + r_{\text{in}})(x_{\text{in}} + r_0(i) + r_{\text{in}})]^{1/2}\}$$

$$\omega_{\text{wake}} = \begin{cases} 1 & \text{if } \mathfrak{R}_{\text{in}_0} \leq \chi^- \leq \mathfrak{I}_{\text{in}_0} \ \& \ y_n - y_i > 0 \\ 1 & \text{if } \mathfrak{R}_{\text{in}_0} \leq \chi^+ \leq \mathfrak{I}_{\text{in}_0} \ \& \ y_n - y_i > 0 \\ 0 & \text{otherwise} \end{cases}$$

(6)

where

$$\begin{aligned} \mathcal{R}_{in_0} &= x_i - r_{in} , & \chi^- &= x_n - r_0(n) \\ \mathcal{I}_{in_0} &= x_i + r_{in} , & \chi^+ &= x_n + r_0(n) \end{aligned}$$

$$v_n = v_0 \left[ 1 - \sqrt{\sum_{i=1}^N \left[ \omega_{wake} A_x \frac{[1 - \sqrt{1 - C_t}]^2}{r} \right]} \right]$$

(7)

## 2.2 Cabling layout design

The importance of optimising the cable routes is not less than the importance of optimising wind turbine siting. Hence, it is advantageous to co-optimize the cable work along with the number and locations of the wind turbines. Selection of the cable must comply with the technical requirements needed to ensure the reliability of the system like the current carrying capacity during normal operation conditions.

Dutta and Overbye in [47] review the different types of cable layouts. The main cable topologies that exist are ring cabling and radial cabling. In this paper, the radial topology is adopted to connect the turbines to the PCC. In this topology, a collector cable is laid straight across the WF, with smaller cables connecting each wind turbine to the main cable through the shortest path possible. This topology is illustrated in Figure 2. The route of the collector cable across the WF is the decision subject in this problem. The cable route is represented by the two parameters of a straight-line Equation (8).

These two parameters are the decision variables of the cable routing problem. The connection point of each turbine's service cable to the main collector cable is a ring main unit (RMU), which also facilitates the protection equipment and isolates a wind turbine for maintenance or protection. The red dashed line represents the main collector cable, with length ( $L_B$ ). The black dashed lines are the small service cables for each wind turbine, each with its own length ( $L_S$ ).

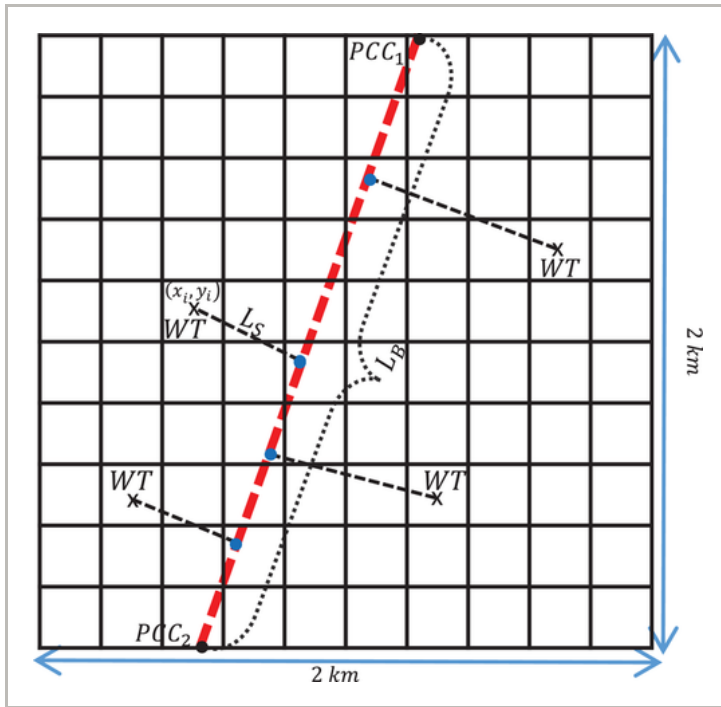


**FIGURE 2** [Open in figure viewer](#) | [PowerPoint](#)

Illustration of cabling connections and PCC model

The main cable is modelled as a straight line characterized by its slope ( $M_{big}$ ) and y-intercept ( $B_{big}$ ) as stated in Equation (8).

$$Y_{main} = M_{big} (x_{PCC1} - x_{PCC2}) + B_{big}$$

(8)

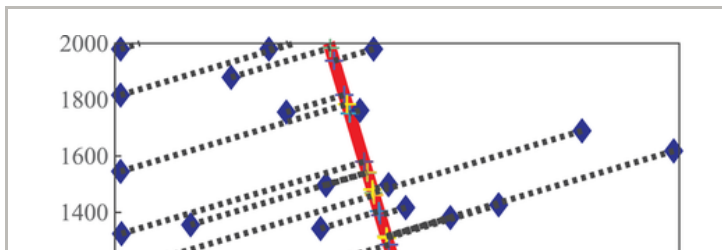
Thus, two intersection points between the main cable and the land's borders are identified as  $PCC_1(x_{PCC1}, y_{PCC1})$  and  $PCC_2(x_{PCC2}, y_{PCC2})$ . The length of the main cable ( $L_B$ ) is calculated using the formula of the distance between two points in Euclidian space.

$$L_B = \sqrt{[(x_{PCC1} - x_{PCC2})^2 + (y_{PCC1} - y_{PCC2})^2]} \quad (9)$$

One service cable is laid for each single wind turbine. The routing of the service cable is determined using the shortest distance between the wind turbine location ( $x_i, y_i$ ) and an intersection in the straight line (i.e. the main cable). This formula is illustrated in Equation (10).

$$L_S = \frac{|M_{big} x_i - y_i + B_{big}|}{\sqrt{(M_{big}^2 + 1)}} \quad (10)$$

For WTs located near the border, this formula leads the service cable to cross outside the land's border. In such cases, the connection point between the service cable and the main cable is adjusted to be the nearest point on the main cable located inside the land. The new length of the service cable is calculated accordingly. This can be observed for the WT at the top and bottom of the farm in Figure 3.





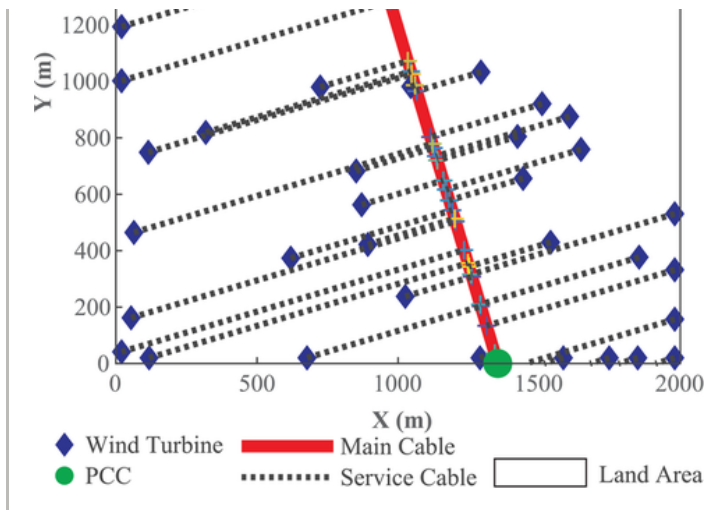


**FIGURE 3** [Open in figure viewer](#) | [↓ PowerPoint](#)

WTs whose service cable extends outside the farm's land lot

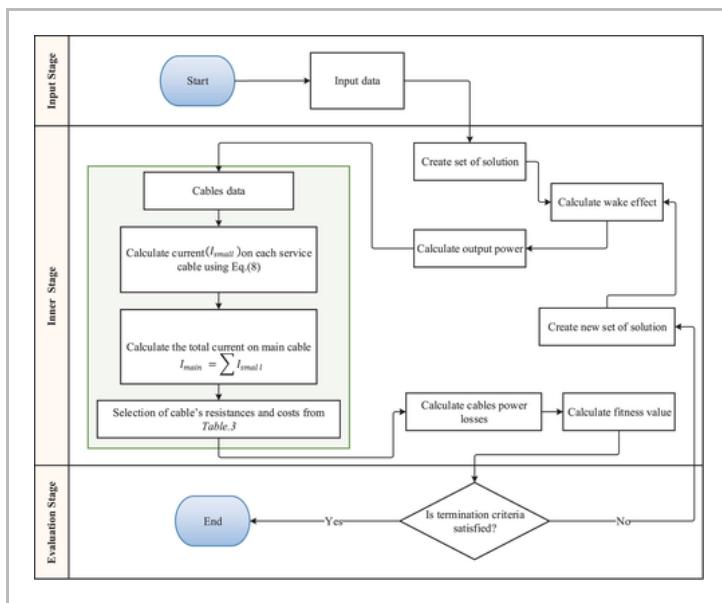
The losses are calculated based on the amount of electrical current flowing through both the main and service cables using Equation (21). The main collector cable intersects with the land's borders at two points. These two points are candidates for serving as the WF's PCC. Either one can be chosen, but not both. Losses on the main cable are calculated for the two candidate PCC points:  $PCC_1$  and  $PCC_2$ . The intersection point corresponding to less expected losses is chosen as the PCC of the WF. While the expected cable losses over all wind scenarios are considered in the objective function, the size of the main collector cable is based on the maximum current flow scenario among all wind scenarios. This maximum current flow scenario is based on the total power output of the wind turbines incorporating the wake effect. Moreover, service cables are sized based on the maximum current of each individual wind turbine over all wind scenarios, incorporating the wake effect as well. A lookup table for cable sizes and maximum current carrying capability is used. The cost of each cable type per unit length is also provided. The current in each service cable ( $I_{sc}$ ) is

provided. The current in each service cable ( $I_{small}$ ) is calculated using Equation (11) as a function of the turbine's power output in each wind scenario. The connection point of each turbine's service cable on the main collector cable divides the main collector cable to segments, such that each segment observes a different current magnitude. Segments of the main cable which are closer to the PCC observe larger current magnitudes. The WTs generate power at a nominal voltage of ( $V_{LL}$ ) and a power factor of  $\cos(\theta)$ . The cable selection process is shown in the whole process for solving WFLO in Figure 4.

$$I_{cable} = \frac{P_{cable}(v_i, \theta, N)}{\sqrt{3}V_{LL} \cos(\theta)} \tag{11}$$

where

$$P_{cable} \in [P_{small}, P_{main}], I_{cable} = [I_{small}, I_{main}]$$



## 2.3 Optimisation problem

The optimal design of a WF is dependent on the location of wind turbines and total length of cable work. The WFLO problem has technical and cost limitations. The objective function is to minimize the cost of energy (CoE). The WF's power output for each wind scenario is weighted by this scenario's probability, and the expected power output is incorporated in the optimisation objective. This section presents the optimisation model to minimize the WF's cost, as a function of WT's number, location, cable layout, and PCC location.

The optimisation model is presented in Equations (12)–(21).

$$\text{Min (CoE)} = \text{Min} \left[ \frac{N \left( \frac{2}{3} + \frac{1}{3} e^{(-0.00174N^2)} \right) \text{cost}_T + \mathcal{C}}{P_{\text{farm}} - \sum_{i=1}^N P_i^{\text{loss}}} \right] \quad (12)$$

subject to

$$D_{\text{in}} = \left\{ \sqrt{[x_i - x_n]^2 + [y_i - y_n]^2} \geq (5D_{r0}) \right. \\ \left. x_i, y_i, x_n, y_n \in \mathcal{S}, \forall i, n = 1, \dots, N, i \neq n \right\} \quad (13)$$

$$0 \leq x_k \leq l \ \& \ 0 \leq y_k \leq w \quad \forall k \in [i, n], \quad l, w = 2000$$

(14)

$$N > 0$$

(15)

$$x_{\text{PCC}_1} \times (w - x_{\text{PCC}_1}) \times y_{\text{PCC}_1} \times (l - y_{\text{PCC}_1}) = 0$$

(16)

$$x_{\text{PCC}_2} \times (w - x_{\text{PCC}_2}) \times y_{\text{PCC}_2} \times (l - y_{\text{PCC}_2}) = 0$$

(17)

$$\sqrt{(x_{\text{PCC}_1} - x_{\text{PCC}_2})^2 + (y_{\text{PCC}_1} - y_{\text{PCC}_2})^2} > 0$$

(18)

where

$$\mathcal{C} = L_B C_B + C_S \sum_{i=1}^N L_S$$

(19)

$$P_{\text{farm}} = \left\{ \begin{array}{l} \sum_{k=0}^{360^\circ} \sum_{i=1}^N [P_i [(x, y), v_{i,\theta_k}] P_r (v_i, \theta_k)] \\ 0 \leq P_r \leq 1, \sum P_r = 1 \end{array} \right\}$$

(20)

$$P_i^{\text{loss}} = \left\{ \left[ \frac{\sum_{k=0}^{\text{DOV}} P_i(v_i, \theta_k) P_r(v_i, \theta_k)}{\sqrt{3} V_{LL} \cos(\theta)} \right]^{-1} \times [R_{S,i} L_{S,i} + R_{B,i} L_{B,i}] \quad i \in \{1, \dots, n\} \right\} \quad (21)$$

The numerator of the objective function in Equation (12) is composed of three terms. The first term corresponds to the cost of wind turbines, and it considers economy of scale [15]. The other two terms correspond to the cost of cable work. The denominator of the objective function represents the net power produced.

The total output power of all wind turbines is defined in Equation (20), as a non-linear function of the turbines' locations (  $x, y$ ) within the farm, the probability of occurrence ( $P_r$ ) of each wind scenario (  $v, \theta$ ). Wind speed ( $v$ ) is calculated using Jensen's wake-effect model given in Equation (7). Turbines which do not fall in the wake-effect cone of any upstream turbines experience the full speed of a wind stream ( $v_0$ ). Losses in the main and service cables are calculated using Equation (21). A minimum clearing distance ( $D_{in}$ ) between two turbines is set for safety distance [9, 48] and is equivalent to five times the turbine's radius. This constraint is described by Equation (13). The other inequality constraints are the terrain's width and length constraint, and the minimum number of turbines in the farm, illustrated by Equations (14) and (15), respectively. The PCC must lie in one of the land's borders where this is presented in Equation (16) for  $PCC_1$  and Equation (17) for  $PCC_2$ . The constraint in Equation (18) forces the locations of  $PCC_1$  and  $PCC_2$  not to be in the same location.

The WFLO problem is non-linear and highly non-convex.

It is computationally expensive to solve such mixed-integer nonlinear problem with analytical algorithms. Therefore, the heuristic optimisation technique GA is used for solving this optimisation problem. The decision variables are locations of wind turbines  $(x, y)$ , and for the cable design part, the slope  $(M_{\text{big}})$  and cable intercept  $(B_{\text{big}})$  of the main cable.

Two design cases are considered:

1. Co-optimisation: Solving of WFLO and cabling connections simultaneously.
2. Separate optimisation: Solving of WFLO and cabling connections sequentially as two separate problems.

The wind turbines layout objective is presented in Equation (22) without cabling items. For the cabling work optimisation, an objective function given by Equation (23) is used to connect all the turbines toward the PCC.

- Wind turbines layout optimisation

$$\text{Fcn}_T = \text{Min} \left[ \frac{N \left( \frac{2}{3} + \frac{1}{3} e^{(-0.00174N^2)} \right) \times \text{cost}_T}{P_{\text{farm}}} \right] \quad (22)$$

subject to Equations (13)–(15)

- Cabling connections optimisation:

$$\text{Fcn}_C = \text{Min} \left[ \frac{L_B C_B + C_S \sum_{i=1}^N L_S}{P_{\text{farm}} - \sum_{i=1}^N P_i^{\text{loss}}} \right] \quad (23)$$

subject to Equations (14),(16)–(18)

The integrated tool will be investigated under a single optimisation scenario, as illustrated in Figure 4. It is divided into three stages: input, inner, and evaluation stages. The input stage involves importing WT design data, terrain property, wind profile, cable properties, and costs of WTs and cables. The inner stage involves the calculation of the main parameters to evaluate a fitness value. The main parameters in the inner stage are calculated in sequence as a single optimisation problem. The last stage, the evaluation stage, involves evaluating the fitness value and making a decision to terminate the optimisation or produce a new candidate solution. The optimisation process stops when the improvement in the fitness value has been below a threshold for a number of consecutive steps or if the maximum number of iterations is reached.

## 2.4 Verification of the wake-effect model

To validate the wake-effect model and the formulation of the optimisation problem, the proposed methodology was benchmarked using the study cases from Grady et al.[15]. In these study cases, the land size is  $2 \times 2$  km, and the grid size is  $10 \times 10$  cells. The grid size of  $10 \times 10$  has been chosen to be able to compare the results to Grady's results. However, higher grid resolution requires more computational effort. The benchmark was carried out for the first two scenarios of Grady's paper, namely, constant wind speed-constant direction and constant wind speed-variable wind direction. To ensure the similarity of the problems, we used the same fitness function as Grady. The results are compared with Grady's in Table 1. Despite, in the present study, different population size and generations

are used compared to Grady's study, the fitness values achieved are slightly better. In the present study, the optimal number of wind turbines for both wind scenarios are 31 and 41 turbines compared to 30 and 39 turbines in [15]. Accordingly, the wind farm generation will be higher that leads to improve the fitness values. Besides, fixed number of turbines are used instead of optimising that. The numbers of turbines ( $N$ ) are 30 and 39 turbines as used in Grady's study. As shown in Table 1, the present results for fixed ( $N$ ) are near to Grady's results. Therefore, the developed model is sufficient to proceed for further analysis.

**TABLE 1.** Present results versus Grady's results

	Fitness value	Total power (kW year)	Turbines (No.)	Generation	Posiz
Constant speed and direction					
Grady's results	0.0015436	14,310	30	3000	60
Present results (optimised $N$ )	0.0015111	14,961	31	100	50
Present results (fixed $N$ )	0.0015059	14,668	30	100	50
Constant speed and variable direction					
Grady's results	0.0015666	17,220	39	3000	60



Present results (optimised N)	0.001472	19,067	41	100	50
-------------------------------	----------	--------	----	-----	----

### 3 CASE STUDY: WIND TURBINES LAYOUT INCLUDING OPTIMAL CABLE DESIGN

A case study is performed to demonstrate the applicability of the proposed methodology. A  $2 \times 2$  km land is chosen as a potential WF site. The site assumed a flat terrain with a surface roughness length ( $z_0$ ) of 0.3 m. The histogram of wind speed and direction for this site at 60 m high is given in Figure 5 [26]. Any change in the wind direction from a predetermined direction will result in a high wake effect that will affect the output power and costs. Thus, the used wind direction is discretised into 36 segments of  $10^\circ$  each with its occurrence probability. As shown in Figure 5, there is a high prevalence of wind directions between  $270^\circ$  and  $360^\circ$ , which means these directions have more effects on the WFLO than other directions. The considered wind speeds in this study are 8, 12, and 17 m/s. The site area is divided into a grid of  $10 \times 10$  cells, with a cell size of  $200 \times 200$  m. Due to land size, smaller wind turbines are used. The properties of the turbines used and site are given in Table 2. The cost of each wind turbine ( $cost_T$ ) is around 554,793 (€/unit), according to the 2017 IRENA report [49]. The cable inventory with the size of each cable, current carrying capacity, and cost is given in Table 3. The WF layout and cabling optimisation problem is solved using the GA in MATLAB software. The results for the co-optimisation of the wind turbines layout and cabling connections are compared with the

separate optimisation of the wind turbines layout and cabling connections.

**TABLE 2.** Parameters used in the study [15]

Rated power [kW]	629	Cut-out speed [m/s]	18
Hub height [m]	60	Wind farm size [km <sup>2</sup> ]	4
Diameter [m]	40	Thrust Coefficient	0.88
Cut-in speed [m/s]	2	Air density [kg/m <sup>3</sup> ]	1.225

**TABLE 3.** Parameters of 33 kV cables used [50]

Cable size	AC resistance ( $\Omega$ /km)	Current carrying capacity (A)	Unit price (€/km)
3C× 50 mm <sup>2</sup>	0.494	181	26,223
3C× 70 mm <sup>2</sup>	0.343	220	32,806
3C× 95 mm <sup>2</sup>	0.247	263	39,115
3C× 120 mm <sup>2</sup>	0.196	298	44,968
3C× 150 mm <sup>2</sup>	0.16	332	51,919
3C× 185 mm <sup>2</sup>	0.128	374	61,884
3C× 240 mm <sup>2</sup>	0.098	431	74,596

\*All cables are XLPE/SWA/PVC 33 KV type.

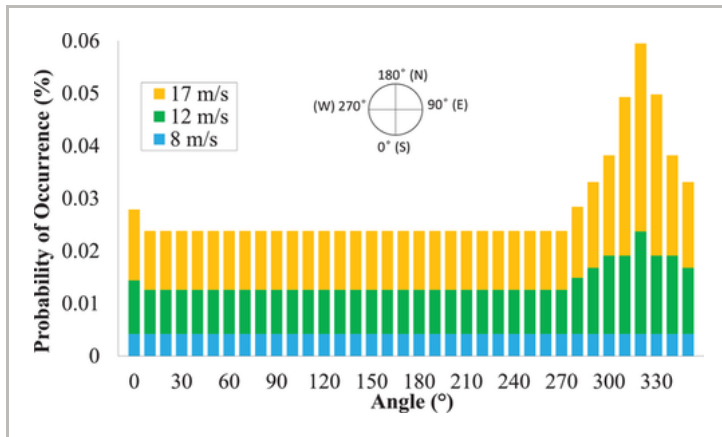


**FIGURE 5** [Open in figure viewer](#) | [PowerPoint](#)

Histogram of wind speed and directions

### 3.1 Results and discussions

The whole problem optimised the wind turbines layout and cabling connections to obtain the optimal power output with minimum power losses. This is achieved by co-optimising the cables and turbine locations together in every population of GA using the objective function for minimising the CoE, as stated in Equation (12). The process for solving the whole WFLO with cabling connections is shown in Figure 4. Running the simulation with the given data produces results of 48 optimal number of turbines which are located primarily on the borders of the WF and in the prevailing wind directions (270–360°). They are mostly distributed on the borders of the WF to reduce the wake effects. Figure 6 shows an example of the wake effects in the farm for wind directions of 0° and 290°. The farm layout is rotated counterclockwise with respect to the south-east coordinate system using the passive

east coordinate system using the passive transformation matrix.

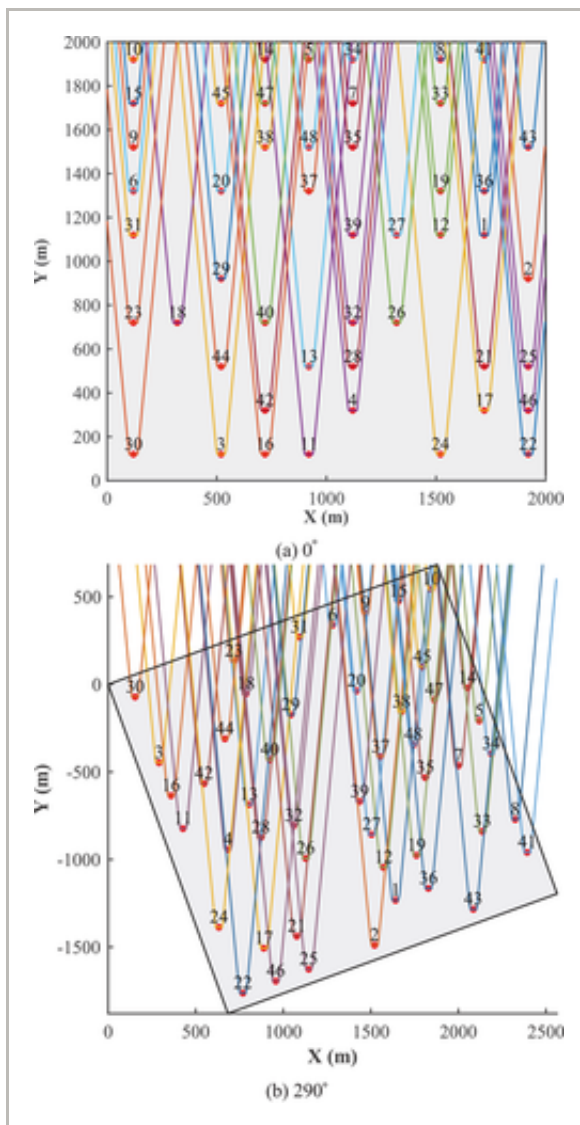


**FIGURE 6** [Open in figure viewer](#) | [↓ PowerPoint](#)

Wind turbines layout with wake-effect cones at different wind directions

This configuration produced a total annual energy of 203.915 GWh with a fitness value of 801.099 €/ kW<sub>year</sub> . The selected cables are 3C × 240 mm<sup>2</sup> for the main one and 3C × 50 mm<sup>2</sup> for the service cables. The lengths of the main cable and service cables are 2.09 and 22.53 km, respectively. Moreover, the losses in the

service cables and main cable are 9.660 and 118.236 MWh, respectively. The two ends of the main cable  $PCC_1$  and  $PCC_2$  have losses of 118.236 and 146.082 MWh; thus,  $PCC_1$  is selected as PCC. The PCC is optimised in the north border of the WF. The ratio of total losses to total generated energy is 0.063%. The WF layout with cabling connections and PCC is presented in Figure 7.

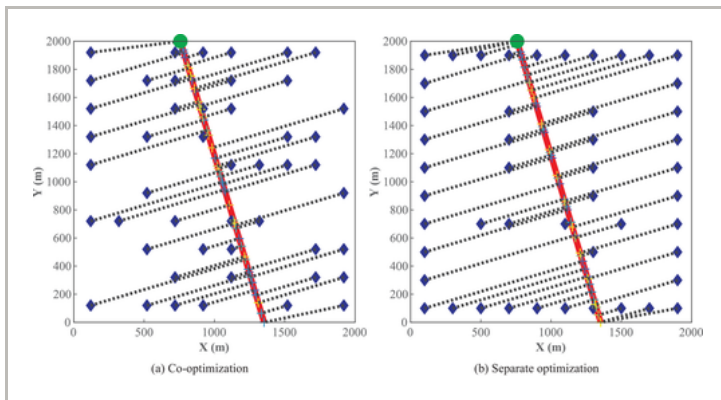


**FIGURE 7** [Open in figure viewer](#) | [PowerPoint](#)

Optimal configuration for the two cases

As mentioned in Section 2.3, to make a comparison between the co-optimisation of WFLO and the separate optimisation for wind turbines locations and cabling connections, the objective functions given by Equation (22) is used for wind turbines siting and Equation (23) for cabling connections. Running the simulation of the separate optimisation gives an overall layout as shown in Figure 7. For the wind turbine layout objective, the fitness value of  $767.631 \text{ €/kW}_{\text{year}}$  has been achieved with a total generated annual energy of 204.038 GWh. In addition, the cabling fitness value is  $37.736 \text{ €/kW}$  with total energy losses of 252.831 MWh. The distances between the wind turbines are higher in an effort to minimize the wake affect among the turbines in the

separate optimization. As a result, the total length of the

separate optimisation. As a result, the total length of the cables reached 29.65 km with 252.831 MWh losses. While using the co-optimised process, the length of the cables reduced to 24.62 km with 127.896 MWh losses. Consequently, the total cable losses for the separate optimisation are higher compared to the co-optimised one by 124.935 MWh. The total losses to the total annual energy represent a percentage of 0.12%. The location of the PCC is optimised in the upper border of the farm.

Table 4 summarises the results of the simulated cases: co-optimisation and separate optimisation. The results provide an indication of the convenience of our integrated approach (co-optimisation) for WFLO and cabling connection instead of optimising each one separately. The comparison of CoE between the two cases shows that the cost of separate optimisation is higher than the co-optimised one by 5.22 €/kW<sub>year</sub>. A lower cost value of turbines is observed in the separate optimisation because the first objective is to separate the turbines far from each other to produce more energy with less wake effect. In terms of annual energy produced, the separate optimisation produced more energy than the co-optimised one by 123 MWh. However, the energy losses due to cabling are higher in the separate optimisation by 124.935 MWh. Thus, the difference ratio between the two cases in terms of the energy losses is about 49.4%.

**TABLE 4.** Comparison of results for the co-optimised and separate cases

	Co-optimisation	Separate optimisation	Difference

Cost of energy with losses (€/kW <sub>year</sub> )_ Equation (12)	801.099	806.319	5.22
Cost of energy without losses (€/kW <sub>year</sub> )_ Equation (22)	769.044	767.631	-1.413
Cost of cables (€/kW)_ Equation (23)	32.055	37.736	5.681
Wind farm annual energy at PCC (GWh)	203.915	204.038	0.123
Cable energy loss (MWh)	127.896	252.831	124.935
No. of turbines	48	48	0
Main cable length (km)	2.09	2.11	0.02

To measure the compactness of the turbines in the farm, the centroid of all the turbines locations in the farm was calculated; then the total average distance from the centroid of the WF to the locations of the turbines was calculated. The centroid of the WF was calculated by averaging the x- and y- coordinates of the turbines locations. The lower average distance means that the turbines are mostly compact near the centroid. The lower average distance from the centroid is found in the co-optimisation, which is expected because it tries to minimize the cable losses and wake effect losses at the same time, in contrast to the separate optimisation. While the difference in the fitness value between the

while the difference in the fitness value between the separate optimisation and co-optimisation is 5.22 €/kW<sub>year</sub>. The difference ratio between the average wind turbines distance to the centroid in the co-optimisation compared with the separate optimisation is 12.49%. It is an indicator that co-optimisation is useful in obtaining a compact WF in a smaller portion of the land.

The effectiveness of the proposed approach is further evaluated in terms of the turbines and cables costs in the farm. A comparison is summarised in Table 5, where the cost of wind turbines is similar in both cases because the same number of turbines is obtained. The cost of cables is calculated by multiplying the cable length with its corresponding cost from Table 3. Consequently, the costs of the main and service cables in the co-optimisation are lower due to the length of cables. In addition, the total cost of constructing the WF using co-optimisation is lower by € 132,776.12. As mentioned before, the difference between the co-optimised and separate cases in terms of annual energy produced is 123 MWh. Using this difference, the British strike price for wind energy of 49.98 €/MWh, and the WF lifetime of 20 years [51] yields a revenue of € 122,950.80, which is less than the difference between the total cost of the two cases. This means even with higher annual energy production in the separate optimisation, the revenue could not compensate the difference in the total capital cost. This result implies that, also in terms of cost, the co-optimisation results are better than the separate ones.

**TABLE 5.** Cost comparison between the co-optimised and separate cases

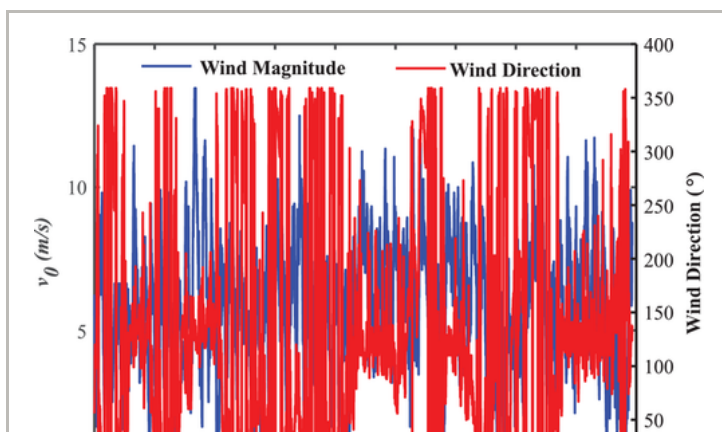
	Co-	Separate	Difference
--	-----	----------	------------



	optimisation	optimisation	
Wind turbines cost [€]	17,901,817.84	17,901,817.84	0
Main cable cost [€]	155,796.33	157,287.21	1,490.88
Service cables cost [€]	590,390.54	721,675.79	131,285.25
Total capital cost [€]	18,648,004.71	18,780,780.83	132,776.12
Revenue [€]	203,833,434	203,956,384.80	122,950.80

## 4 CASE STUDY, SOUTH OF OMAN

To evaluate the WFLO with and without cabling, a comparison is conducted in terms of the wind farm generation. Trying to make the comparison more realistic, a 2-months wind profile in 10-min bases shown in Figure 8 is used. This wind profile pertains to a site located at Thumrait in the Sultanate of Oman. All the other parameters including the WF layout used in the sensitivity analysis are similar to the case study in the previous section.



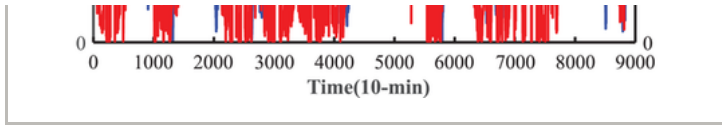


**FIGURE 8** [Open in figure viewer](#) | [↓PowerPoint](#)

Actual 2-month wind profile

Running the simulation yields a total energy of 3.8580 GWh for WF with cabling and 4.5317 GWh for WF without cabling. These outputs are presented with the difference in Figure 9. As noticed, the actual output of WF with cabling is lower compared to the WF without cabling. These results reflecting the co-optimisation and separate optimisation outputs yielded in the above section. Therefore, a decision for including the cabling in the WFLO problem yields a more compacted WF which decreases the WF generation due to the wake losses. There is a total velocity deficit is 16.55% and 10.63% for WF with cabling and WF without cabling, respectively. But, on the other side, the capital cost of the WF is lower due to the shorter cables' lengths.

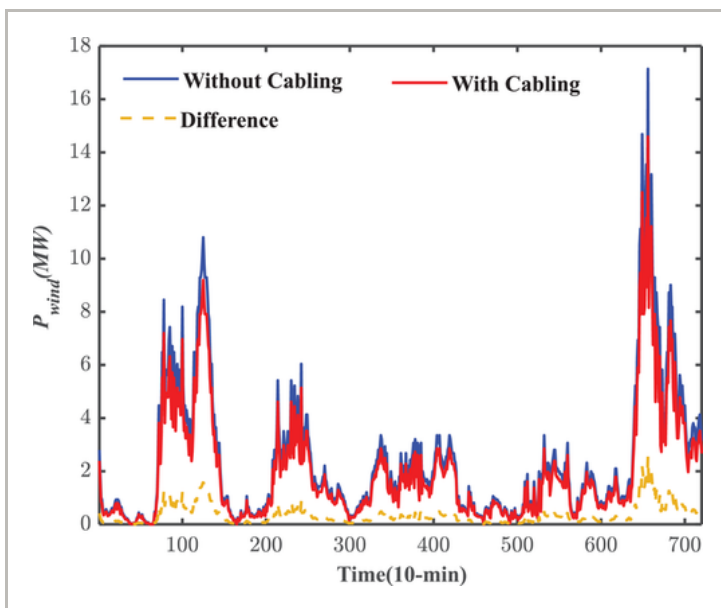


**FIGURE 9** [Open in figure viewer](#) | [↓PowerPoint](#)

Sample of 5-day WF generation

## 5 CONCLUSION

This paper focused on illustrating the significance of developing an appropriate integrated tool to design a WF. Different constraints and parameters, including Jensen's wake effect and cable power active losses, were considered while optimising the overall WF layout. Jensen's wake-effect model was implemented and compared with previous studies to cross-check the results. Magnitude and direction of wind speed are the main factors that are utilized to mimic a real wind scenario. The factors included in this study were, but not limited to, wind direction, wind speed, site terrain, turbine characteristics, and minimum spacing between turbines. The wind profile is a natural phenomenon that cannot be changed. Thus, allocating the turbines in the WF and selecting the well-fit turbine characteristics are the significant factors to reduce wake losses.

Two optimisation cases were evaluated in a case study with multi-speed and multi-direction using GA to achieve maximum annual energy production with minimum wake-effect losses and cable active power losses. The main and service cable connections were optimised to obtain optimal cable losses. The developed approach yielded an output to obtain the optimal wind turbine locations, cabling routes, and PCC. Co-optimisation provided better results than separate optimisation in terms of cable power losses, capital cost, and compactness. While separate optimisation provide better results in terms of annual energy production. To emphasize these results, a comparison between the co-optimisation and separate optimisation in terms of the wind farm generation has been conducted by using a

real multi-speed and multi-direction wind profiles derived from historical 10 min resolution wind speed and direction of a site in Oman.

Thus, this integrated tool is adequate and can be used in the planning stage to perform a feasibility study of the project that considers the economic and technical aspects. The total cost and annual energy output are used to justify the superiority of the co-optimisation approach for wind turbine layout and cabling connections instead of separate optimisation. The lower average wind turbines distance to the centroid emphasizes the usefulness of co-optimisation in utilizing the WF area effectively.

## ACKNOWLEDGMENTS

The authors would like to acknowledge the support of the Sultan Qaboos University, Oman Rural Areas Electricity Company, and HMTF project code (SR/ENG/ECE/17/01).

## NOMENCLATURE

$U_n$	wind speed at position $n$ (m/s)
$v_0$	free stream wind speed (m/s)
$a$	axial induction factor
$\alpha$	decay constant
$C_t$	thrust coefficient
$y_{in}$	distance along the wind direction between turbines $i$ and $n$ (m)

$x_{in}$   
perpendicular distance along the wind direction  
between turbines  $i$  and  $n$  (m)

$T_n$   
downstream wind turbine

$P_{farm}$   
total output power (MW)

$S$   
wind farm space

$P_g$   
generated power from each turbine (MW)

$V_{LL}$   
line-to-line voltage (kV)

$R_s$   
service cable resistance (  $\Omega/\text{km}$  )

$P_i^{\text{loss}}$   
total power losses due to turbine  $i$  (MW)

$L_B$   
length of main cable (m)

$r_{in}$   
wake radius (m)

$r_0$   
downstream rotor radius (m)

$H_{wt}$   
turbine hub height (m)

$z_0$   
surface roughness length (m)

$N$   
number of wind turbines

$\hbar$   
overlapping area of wake and a rotor (  $\text{m}^2$  )

$T_i$   
upstream wind turbine

$\theta$   
wind direction angle (degree)

$P_r$	probability of occurrence (%)
$D_{r0}$	downstream rotor diameter (m)
$R_b$	main cable resistance ( $\Omega/\text{km}$ )
$C_s$	cost of service cable ( $\text{€}/\text{km}$ )
$C_B$	cost of main cable( $\text{€}/\text{km}$ )
$\text{cost}_T$	cost of a wind turbine ( $\text{€}/\text{unit}$ )
$L_s$	length of service cable (m)

## REFERENCES



1 Belu, R., Koracin, D.: Effects of complex wind regimes and meteorological parameters on wind turbine performances. In: 2012 IEEE Energytech, pp. 1– 6. IEEE, Piscataway, NJ (2012)

[Google Scholar](#)

2 Han, X., Guo, J., Wang, P.: Adequacy study of a wind farm considering terrain and wake effect. *IET Gener. Transm. Distrib.* **6**(10), 1001– 1008 (2012)

[Crossref](#) | [Web of Science®](#) | [Google Scholar](#)

3 González, J. S., Payán, M. B., Santos, J. M. R., González-Longatt, F.: A review and recent developments in the optimal wind-turbine micro-siting problem. *Renewable Sustainable Energy Rev.* **30**, 133– 144 (2014)

[Crossref](#) | [Web of Science®](#) | [Google Scholar](#)

4 Hou, P., Zhu, J., Ma, K., Yang, G., Hu, W., Chen, Z.: A review of offshore wind farm layout optimization and electrical system design methods. *J. Mod. Power Syst.*

*Clean Energy* 7(5), 975– 986 (2019)

[Crossref](#) | [Web of Science®](#) | [Google Scholar](#)

---

5 Hou, P., Hu, W., Zhang, B., Soltani, M., Chen, C., Chen, Z.: Optimised power dispatch strategy for offshore wind farms. *IET Renewable Power Gener.* **10**(3), 399– 409 (2016)

[Wiley Online Library](#) | [Web of Science®](#) | [Google Scholar](#)

---

6 Rao, S.S.: *Engineering Optimization: Theory and Practice*. Wiley, New York (2009)

[Wiley Online Library](#) | [Google Scholar](#)

---

7 Shakoor, R., Hassan, M.Y., Raheem, A., Wu, Y.-K.: Wake effect modeling: A review of wind farm layout optimization using jensen's model. *Renewable Sustainable Energy Rev.* **58**, 1048– 1059 (2016)

[Crossref](#) | [Web of Science®](#) | [Google Scholar](#)

---

8 Carbajo Fuertes, F., Markfort, C. D., Porté-Agel, F.: Incoming wind and wake measurements of a single 2.5 MW wind turbine using two nacelle-mounted wind lidars for analytical wake model validation. In: 23rd Symposium on Boundary Layers and Turbulence, Oklahoma City, OK, 11–15 June 2018

[Google Scholar](#)

---

9 Parada, L., Herrera, C., Flores, P., Parada, V.: Wind farm layout optimization using a gaussian-based wake model. *Renewable Energy* **107**, 531– 541 (2017)

[Crossref](#) | [Web of Science®](#) | [Google Scholar](#)

---

10 Politis, E.S., Prospathopoulos, J., Cabezon, D., Hansen, K.S., Chaviaropoulos, P., Barthelmie, R.J.: Modeling wake effects in large wind farms in complex terrain: the problem, the methods and the issues. *Wind Energy* **15**(1), 161– 182 (2012)

[Wiley Online Library](#) | [Web of Science®](#) | [Google Scholar](#)

---

11 Jensen, N.O.: *A Note on Wind Generator Interaction*. Risø National Laboratory, Roskilde (1983)  
[Google Scholar](#)

---

12 Larsen, G.C.: *A Simple Wake Calculation Procedure*. Risø National Laboratory, Roskilde (1988)  
[Google Scholar](#)

---

13 Frandsen, S.: On the wind speed reduction in the center of large clusters of wind turbines. *J. Wind Eng. Ind. Aerodyn.* **39**(1-3), 251– 265 (1992)  
[Crossref](#) | [Web of Science®](#) | [Google Scholar](#)

---

14 Moseetti, G., Poloni, C., Diviacco, B.: Optimization of wind turbine positioning in large windfarms by means of a genetic algorithm. *J. Wind Eng. Ind. Aerodyn.* **51**(1), 105– 116 (1994)  
[Crossref](#) | [Web of Science®](#) | [Google Scholar](#)

---

15 Grady, S., Hussaini, M., Abdullah, M.M.: Placement of wind turbines using genetic algorithms. *Renewable Energy* **30**(2), 259– 270 (2005)  
[Crossref](#) | [Web of Science®](#) | [Google Scholar](#)

---

16 Tang, X., Yang, Q., Wang, K., Stoevesandt, B., Sun, Y.: Optimisation of wind farm layout in complex terrain via mixed-installation of different types of turbines. *IET Renewable Power Gener.* **12**(9), 1065– 1073 (2018)  
[Wiley Online Library](#) | [Web of Science®](#) | [Google Scholar](#)

---

17 Wang, Y., Liu, H., Long, H., Zhang, Z., Yang, S.: Differential evolution with a new encoding mechanism for optimizing wind farm layout. *IEEE Trans. Ind. Inf.* **14**(3), 1040– 1054 (2018)  
[Crossref](#) | [Web of Science®](#) | [Google Scholar](#)

---

18 Ge, M., Wu, Y., Liu, Y., Li, Q.: A two-dimensional model based on the expansion of physical wake boundary for wind-turbine wakes. *Appl. Energy* **233**, 975– 984 (2019)



19 Abdelsalam, A.M., El-Shorbagy, M.: Optimization of wind turbines siting in a wind farm using genetic algorithm based local search. *Renewable Energy* **123**, 748–755 (2018)

[Crossref](#) | [Web of Science®](#) | [Google Scholar](#)

---

20 Al Busaidi, A.S., Kazem, H.A., Al-Badi, A.H., Khan, M.F.: A review of optimum sizing of hybrid pv-wind renewable energy systems in oman. *Renewable Sustainable Energy Rev.* **53**, 185– 193 (2016)

[Crossref](#) | [Web of Science®](#) | [Google Scholar](#)

---

21 Veeramachaneni, K., Wagner, M., O'Reilly, U.-M., Neumann, F.: Optimizing energy output and layout costs for large wind farms using particle swarm optimization. In: IEEE Congress on Evolutionary Computation (CEC), 2012, pp. 1– 7. IEEE, Piscataway, NJ (2012)

[Google Scholar](#)

---

22 Chowdhury, S., Zhang, J., Messac, A., Castillo, L.: Unrestricted wind farm layout optimization (uwflo): Investigating key factors influencing the maximum power generation. *Renewable Energy* **38**(1), 16– 30 (2012)

[Crossref](#) | [Web of Science®](#) | [Google Scholar](#)

---

23 Wagner, M., Day, J., Neumann, F.: A fast and effective local search algorithm for optimizing the placement of wind turbines. *Renewable Energy* **51**, 64– 70 (2013)

[Crossref](#) | [Web of Science®](#) | [Google Scholar](#)

---

24 Kusiak, A., Song, Z.: Design of wind farm layout for maximum wind energy capture. *Renewable Energy* **35**(3), 685– 694 (2010)

[Crossref](#) | [Web of Science®](#) | [Google Scholar](#)

---

25 MirHassani, S.A., Yarahmadi, A.: Wind farm layout optimization under uncertainty. *Renewable Energy* **107**, 288– 297 (2017)

26 Gao, X., Yang, H., Lin, L., Koo, P.: Wind turbine layout optimization using multi-population genetic algorithm and a case study in hong kong offshore. *J. Wind Eng. Ind. Aerodyn.* **139**, 89– 99 (2015)

27 Ulku, I., Alabas-Uslu, C.: A new mathematical programming approach to wind farm layout problem under multiple wake effects. *Renewable Energy* **136**, 1190–1201 (2019).

28 Eroğlu, Y., Seçkiner, S.U.: Design of wind farm layout using ant colony algorithm. *Renewable Energy* **44**, 53– 62 (2012)

29 Amaral, L., Castro, R.: Offshore wind farm layout optimization regarding wake effects and electrical losses. *Engineering Applications of Artificial Intelligence* **60**, 26– 34 (2017)

30 Khare, V., Nema, S., Baredar, P.: Solar–wind hybrid renewable energy system: A review. *Renewable Sustainable Energy Rev.* **58**, 23– 33 (2016)

31 Barszcz, T., Bielecka, M., Bielecki, A., Wójcik, M.: Wind speed modelling using weierstrass function fitted by a genetic algorithm. *J. Wind Eng. Ind. Aerodyn.* **109**, 68– 78 (2012)

32 Shakoor, R., Hassan, M.Y., Raheem, A., Wu, Y.-K.: Wake effect modeling: A review of wind farm layout optimization using Jensen's model. *Renewable Sustainable Energy Rev.* **58**, 1048– 1059 (2016)

33 Bak, T., Graham, A., Saponova, A., Florian, M., Dalsgaard Sørensen, J., Knudsen, T., Hou, P., Chen, Z.: Baseline layout and design of a 0.8 gw reference wind farm in the north sea. *Wind Energy* **20**(9), 1665– 1683 (2017)

[Wiley Online Library](#) | [Web of Science®](#) | [Google Scholar](#)

---

34 Nandigam, M., Dhali, S.K.: Optimal design of an offshore wind farm layout. In: 2008 International Symposium on Power Electronics, Electrical Drives, pp. 1470– 1474. IEEE, Piscataway, NJ (2008)

[Google Scholar](#)

---

35 Jenkins, A., Scutariu, M., Smith, K.: Offshore wind farm inter-array cable layout. In: 2013 IEEE Grenoble Conference, pp. 1– 6, IEEE, Piscataway, NJ (2013)

[Google Scholar](#)

---

36 Song, M., Chen, K., He, Z., Zhang, X.: Optimization of wind farm micro-siting for complex terrain using greedy algorithm. *Energy* **67**, 454– 459 (2014)

[Crossref](#) | [Web of Science®](#) | [Google Scholar](#)

---

37 Wędzik, A., Siewierski, T., Szypowski, M.: A new method for simultaneous optimizing of wind farm's network layout and cable cross-sections by milp optimization. *Appl. Energy* **182**, 525– 538 (2016)

[Crossref](#) | [Web of Science®](#) | [Google Scholar](#)

---

38 Hou, P., Hu, W., Chen, C., Chen, Z.: Optimisation of offshore wind farm cable connection layout considering levelised production cost using dynamic minimum spanning tree algorithm. *IET Renewable Power Gener.* **10**(2), 175– 183 (2016)

[Wiley Online Library](#) | [Web of Science®](#) | [Google Scholar](#)

---

39 Gonzalez-Longatt, F.M., Wall, P., Regulski, P., Terzija, V.: Optimal electric network design for a large offshore wind farm based on a modified genetic algorithm approach. *IEEE Syst. J.* **6**(1), 164– 172 (2012)  
[Crossref](#) | [Web of Science®](#) | [Google Scholar](#)

---

40 Zhao, M., Chen, Z., Blaabjerg, F.: Optimisation of electrical system for offshore wind farms via genetic algorithm. *IET Renewable Power Gener.* **3**(2), 205– 216 (2009)  
[Crossref](#) | [Web of Science®](#) | [Google Scholar](#)

---

41 Luo, H., Hu, Z., Ning, J., Jiang, C., Niu, S., Yang, J.: A fully distributed reactive power controller for a wind farm to minimize power losses. In: 2018 53rd International Universities Power Engineering Conference (UPEC), pp. 1– 6, IEEE, Piscataway, NJ (2018)  
[Google Scholar](#)

---

42 Lehmann, S., Rutter, I., Wagner, D., Wegner, F.: A simulated-annealing-based approach for wind farm cabling. In: Proceedings of the Eighth International Conference on Future Energy Systems, pp. 203– 215, ACM Press, New York (2017)  
[Google Scholar](#)

---

43 Fischetti, M., Pisinger, D.: Optimal wind farm cable routing: Modeling branches and offshore transformer modules. *Networks* **72**(1), 42– 59 (2018)  
[Wiley Online Library](#) | [Web of Science®](#) | [Google Scholar](#)

---

44 Fischetti, M., Pisinger, D.: Optimizing wind farm cable routing considering power losses. *Eur. J. Oper. Res.* **270**(3), 917– 930 (2018)  
[Crossref](#) | [Web of Science®](#) | [Google Scholar](#)

---

45 Peña, A., Réthoré, P., van der Laan, M.P.: On the application of the jensen wake model using a turbulence-dependent wake decay coefficient: the

sexdierum case. *Wind Energy* 19(4), 163– 176 (2016)

[Wiley Online Library](#) | [Web of Science®](#) |

[Google Scholar](#)

---

46 Moskalenko, N., Rudion, K., Orths, A.: Study of wake effects for offshore wind farm planning. In: 2010

Modern Electric Power Systems, pp. 1– 7, IEEE,

Piscataway, NJ (2010)

[Google Scholar](#)

---

47 Dutta, S., Overbye, T.: A clustering based wind farm collector system cable layout design. In: 2011 IEEE Power and Energy Conference, pp. 1– 6, IEEE, Piscataway, NJ (2011)

[Google Scholar](#)

---

48 Chen, Y., Li, H., Jin, K., Song, Q.: Wind farm layout optimization using genetic algorithm with different hub height wind turbines. *Energy Convers. Manage.* **70**, 56– 65 (2013)

[Crossref](#) | [PubMed](#) | [Web of Science®](#) |

[Google Scholar](#)

---

49 Kieffer, G., Couture, T.D.: *Renewable Energy Target Setting*. International Renewable Energy Agency, Abu Dhabi (2015)

[Google Scholar](#)

---

50 Industry, O.C.: Cables Cost,

<http://www.omancables.com> . Accessed 15 May 2019

[Google Scholar](#)

---

51 Bunn, D.W., Muñoz, J.I.: Supporting the externality of intermittency in policies for renewable energy. *Energy Policy* **88**, 594– 602 (2016)

[Crossref](#) | [Web of Science®](#) | [Google Scholar](#)

Copyright (2021) The Institution of Engineering and Technology. The Institution of Engineering and Technology is registered as a Charity in England & Wales (no 211014) and Scotland (no SC038698)

[About Wiley](#)  
[Online Library](#)

[Privacy Policy](#)

[Terms of Use](#)

[Cookies](#)

[Accessibility](#)

[Help &  
Support](#)

[Contact Us](#)

[Training and  
Support](#)

[DMCA &  
Reporting Piracy](#)

[Opportunities](#)

[Subscription  
Agents](#)

[Advertisers &  
Corporate  
Partners](#)

[Connect with  
Wiley](#)

[The Wiley  
Network](#)

[Wiley Press Room](#)